

Title	Dual wave farms for energy production and coastal protection under sea level rise
Authors	Rodriguez-Delgado, Cristobal;Bergillos, Rafael J.;Iglesias, Gregorio
Publication date	2019-03-09
Original Citation	Rodriguez-Delgado, C., Bergillos, R. J. and Iglesias, G. (2019) 'Dual wave farms for energy production and coastal protection under sea level rise', Journal of Cleaner Production, 222, pp. 364-372. doi: 10.1016/j.jclepro.2019.03.058
Type of publication	Article (peer-reviewed)
Link to publisher's version	http://www.sciencedirect.com/science/article/pii/S0959652619307474 - 10.1016/j.jclepro.2019.03.058
Rights	© 2019, Elsevier Ltd. All rights reserved. This manuscript version is made available under the CC BY-NC-ND 4.0 license. - https://creativecommons.org/licenses/by-nc-nd/4.0/
Download date	2024-04-17 04:13:20
Item downloaded from	https://hdl.handle.net/10468/7740

Dual wave farms for energy production and coastal protection under sea level rise

Cristobal Rodriguez-Delgado^{a,b}, Rafael J. Bergillos^{c,*}, Gregorio Iglesias^{d,a}

^a*School of Engineering, University of Plymouth, Plymouth PL4 8AA, UK*

^b*PROES Consultores, Calle San Germán 39, 28020 Madrid, Spain*

^c*Hydraulic Engineering Area, Department of Agronomy, University of Córdoba, Campus Rabanales, Leonardo Da Vinci Building, 14071 Córdoba, Spain*

^d*MaREI, Environmental Research Institute & School of Engineering, University College Cork, College Road, Cork, Ireland*

Abstract

Climate change is poised to exacerbate coastal erosion. Recent research has presented a novel strategy to tackle this issue: dual wave farms, i.e., arrays of wave energy converters with the dual function of carbon-free energy generation and coastal erosion mitigation. However, the implications of sea level rise – another consequence of climate change – for the effectiveness of wave farms as coastal defence elements against shoreline erosion have not been studied so far. The objective of this work is to investigate how the coastal defence performance of a dual wave farm is affected by sea level rise through a case study (Playa Granada, southern Iberian Peninsula). To this end, a spectral wave propagation model, a longshore sediment transport formulation and a one-line model are combined to obtain the final subaerial beach areas for three sea level rise scenarios: the present situation, an optimistic and a pessimistic projection. These scenarios were modelled with and without the wave farm to assess its effects. We find that the dual wave farm reduces erosion and promotes accretion regardless of the sea level rise scenario considered. In the case of westerly storms, the dual wave farm is particularly effective: erosion is transformed into accretion. In general, and importantly, sea level rise strengthens the effectiveness of the dual wave farm

*Corresponding author.

E-mail address: rafael.bergillos@uco.es (R.J. Bergillos)

as a coastal protection mechanism. This fact enhances the competitiveness of wave farms as coastal defence elements.

Keywords: Renewable energy; Wave energy; climate change; sea level rise; coastal protection; sustainable development

1. Introduction

The large-scale exploitation of fossil fuels that started with the Industrial Revolution has caused serious environmental repercussions [1–4], including sea level rise and climate change [5, 6]. One of the most important challenges in the 21st century is to mitigate these repercussions in as much as possible, not least by developing new kinds of sustainable, carbon-free energies [7–19]. In this sense, ocean energies, and wave energy in particular, stand out as one of the most important due to the high resource availability [20–22].

Previous research in wave energy has focused on different aspects related to its exploitation: (i) the development of new technologies [23–29], (ii) the availability of the resource [30–37], (iii) synergies with other types of offshore renewable energies [38–40] and (iv) economic aspects [41–44]. However, the relation between this kind of technology and the incoming sea level rise still needs further research work if wave energy is going to be poised as a functional carbon-free energy in the near future.

Future sea level rise is becoming a threat for coasts across the world, increasing hazards like coastal flooding [45–47]. Among them, coasts near river deltas are being primarily affected, since they allocate places with high economic, social and environmental importance. In addition, anthropogenic interventions on their catchment areas are increasing other hazards as coastal erosion [48, 49].

One of the advantages of wave farms, i.e. arrays of wave energy converters (WECs), is the reduction in wave power in their lee. When waves are transmitted through the farm, part of their energy is absorbed. On these grounds, wave farms can be used to mitigate coastal erosion [50–55] and flooding [56]. In fact, dual wave farms have been defined as those designed to fulfil both functions:

carbon-free energy generation and coastal defence [57, 58]. Nevertheless, the wave farm effects on longshore sediment transport (LST), shoreline evolution and dry beach area availability under sea level rise have not been analyzed so far. This analysis is necessary and relevant since sea level rise is one of the most dangerous consequences of climate change and induces changes on wave propagation and sediment transport patterns.

The objective of this work is to investigate the effects of sea level rise on the functionality of a wave farm for coastal protection against shoreline erosion. To this end, three sea level scenarios were analysed: the present situation (baseline), and the water level in 2100 according to optimistic (RCP4.5) and pessimistic (RCP8.5) projections proposed by [5]. A third-generation wave propagation model (SWAN) was applied to two case studies, with and without a wave farm, on a gravel dominated beach: Playa Granada (Southern Iberian Peninsula). The evolution of the shoreline was computed using a LST formulation [59] and a one-line model [60] in order to obtain the variations in subaerial beach area. The following sections describe the study area (Section 2), methodology (Section 3), results (Section 4), discussion (Section 5) and conclusions (Section 6) of this work.

2. Study area

Playa Granada is a 3-km-long beach located on the southern coast of Spain that faces the Mediterranean Sea (Figure 1). The beach corresponds to the central stretch of the Guadalfeo deltaic coast and is bounded to the west by the Guadalfeo River mouth and to the east by *Punta del Santo*, the former location of the river mouth [61, 62]. The deltaic coast is bounded to the west by Salobreña Rock and to the east by Motril Port.

The state of the beach profile is practically reflective and the morphodynamic response of the beach is dominated by the gravel fraction [63, 64]. The studied stretch of beach has been experiencing shoreline retreat and terminal erosion in recent years (Fig. 1c), partly due to anthropogenic interventions in the

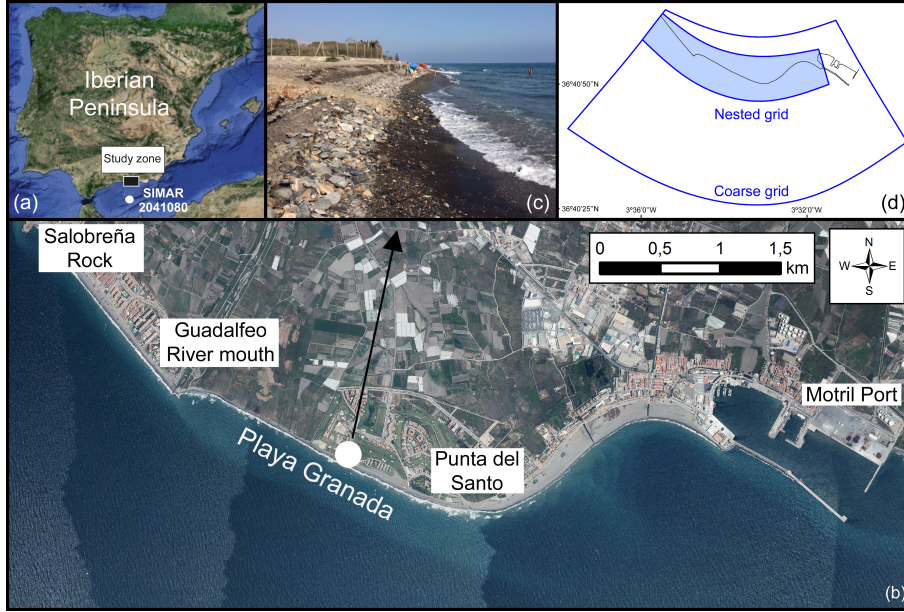


Figure 1: (a) Location of the study site in the southern part of the Iberian Peninsula. (b) Aerial photograph of the study site, including the locations of the main geographical features and structures. (c) Storm erosion in Playa Granada. (d) Computational domains used in the numerical model.

55 Guadalfeo River basin [61, 65]. As a result, artificial nourishment projects
 56 have been frequently performed over the past decade [66], but the long-term
 57 efficiency of these projects has been very limited [67, 68].

58 The region is subjected to the passage of extra-tropical Atlantic cyclones
 59 and Mediterranean storms [69]. The storm wave climate is distinctly bimodal
 60 with the prevailing west-southwest (extra-tropical cyclones) and east-southeast
 61 (Mediterranean storms) wave directions [70]. Peak significant wave heights dur-
 62 ing typical and extreme storm events exceed 2.1 m and 3.1 m, respectively
 63 [71]. The astronomical tidal range is ~ 0.6 m (micro-tidal conditions), whereas
 64 typical storm surge levels can exceed 0.5 m [63].

3. Materials and methods

3.1. Modelled wave farm

The influence of wave energy extraction on the wave propagation and sediment transport of Playa Granada was studied modelling a wave farm off the coast, near Punta del Santo (Fig. 2). This wave farm was composed by eleven WECs, arranged in two rows. The location and layout of the wave farm were chosen based on the optimization for coastal defence purposes carried out in previous works [53, 54].

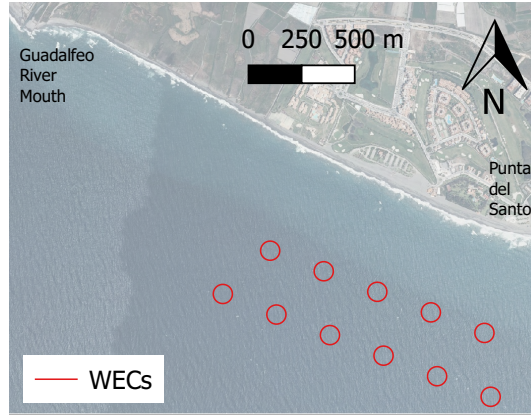


Figure 2: Wave farm location in front of Playa Granada.

The wave energy converter (WEC) selected for the analysis was WaveCat [72, 73]. This device, shown in Figure 3, is a floating and overtopping WEC that comprises two hulls joined by a hinge at the stern [73–75]. For a detailed description of the device, the reader is referred to [25, 76]. Wave farms consisting of WaveCat WECs have been proven to fulfil the dual function of wave energy generators and coastal defence (e.g., Rodriguez-Delgado et al. [57], Abanades et al. [58], among others). This device was included in the wave propagation numerical model through its transmission and reflection coefficients [25]. The inter-device spacing was set to $2D$, with $D = 90$ m the diameter of WaveCat. In order to properly investigate the effects of the wave farm, the baseline (no wave farm) situation was also analysed.

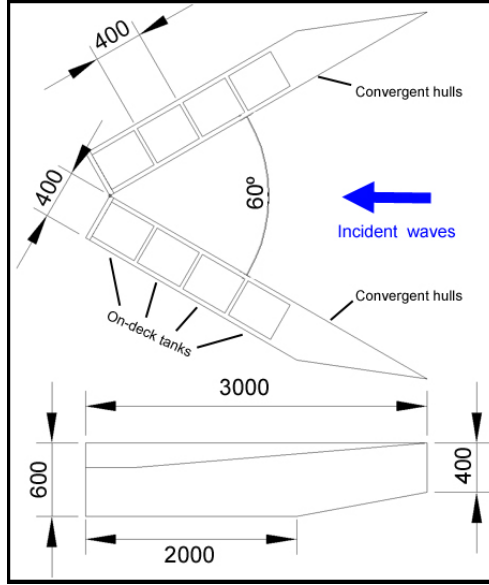


Figure 3: Geometry of the WaveCat device at a 1:30 scale (dimensions in mm).

3.2. Wave and water level conditions

The response of the shoreline was modelled at the storm time scale; more specifically, two sea states were studied, corresponding to westerly and easterly storms – the two prevailing wave directions at the study site. The most frequent values of significant wave height and peak period for storm conditions were selected (Table 1).

Table 1: Parameters of the sea states. [H_s : significant wave height, T_p : peak period, θ : mean wave direction].

	H_s (m)	T_p (s)	θ ($^\circ$)
West	3.1	8.4	238
East	3.1	8.4	107

These sea states were applied to three scenarios: the present situation (SLR0), and the optimistic (SLR1) and pessimistic projections (SLR2) of sea level rise in 2100, according to the representative concentration pathways (RCP) 4.5 and 8.5 proposed by [5] for the study site.

94 3.3. Wave propagation model

95 The influence of wave farm and sea level rise in the wave field was computed
96 by means of the third-generation wave propagation model SWAN [77]. This
97 numerical model is able to simulate the effects of obstacles on wave propaga-
98 tion patterns, i.e., reduction of the wave height propagating behind or over the
99 obstacle along its length, reflection of the waves that impinge the obstacle, and
100 diffraction of the waves around its boundaries [37, 78, 79].

101 The WaveCat WECs were thus included as obstacles in the numerical model,
102 using transmission and reflection coefficients obtained in laboratory experiments
103 [25]. Two computational grids were used (Fig. 1): (i) a coarse grid, covering
104 the region from deep water to the nearshore, with cell sizes that decrease with
105 depth from 170x65 m to 80x80 m; and (ii) a nested grid, covering the inshore
106 region and wave farm area, with cell sizes of approximately 25x15 m. The cell
107 size of the nested grid was adjusted to reproduce properly the effects of each
108 WEC.

109 The spectral resolution of the frequency space consisted of 37 logarithmically
110 distributed frequencies ranging from 0.03 to 1 Hz. For the directional space,
111 the 360° were covered by 72 directions in increments of 5°. This model was
112 previously calibrated and validated in the study area using data from extensive
113 field campaigns [67]. SWAN results were used to obtain wave parameters at
114 breaking, which are the basis of the LST formulation.

115 3.4. LST formulation and one-line model

116 LST rates in the study site for each sea level rise scenario, with and without
117 wave farm, were computed using the formulation of [59] (Eq. 1). This equation
118 has been proved to provide accurate results in a wide range of beach types, from
119 sandy to gravel beaches. More to the point, it has been applied in the study site
120 and successfully validated against field data [67]. The formula can be expressed
121 as follows:

$$Q = 0.00018 K_{swell} \rho_s g^{0.5} (\tan \beta)^{0.4} (d_{50})^{-0.6} (H_{s,br})^{3.1} \sin(2\theta_{br}), \quad (1)$$

122 where Q stands for the LST rate, $\rho_s = 2650 \text{ kg/m}^3$ is the sediment density,
 123 $g = 9.81 \text{ m/s}^2$ the acceleration of gravity, $d_{50} = 0.02 \text{ m}$ the sediment size, $\tan \beta$
 124 the slope of the surf zone, $H_{s,br}$ the significant wave height at the breaking line,
 125 θ_{br} the mean wave direction at breaking and K_{swell} is a parameter which takes
 126 into account the effect of the wave period and varies between 1 and 1.5. This
 127 formulation was applied to compute LST rates for 341 beach profiles, evenly
 128 distributed, covering the stretch of coast between Salobreña Rock and Motril
 129 Port (Fig. 1).

130 The LST rates obtained were used to track changes in the shoreline posi-
 131 tion of each beach profile using the one-line model [60]. As in the case of the
 132 LST formulation, this model has been applied successfully to the study site in
 133 previous works [67]. The model equation is:

$$\frac{\partial y_s}{\partial t} = \frac{1}{D} \left(\frac{-\partial Q}{\partial x_s} \right), \quad (2)$$

134 with y_s and x_s the position of the shoreline, t the time, and D a repre-
 135 sentative length, taken as the summation of the berm height and the depth of
 136 closure.

137 4. Results

138 4.1. Wave farm interaction with the wave field

139 The changes in significant wave height at breaking, $H_{s,br}$, caused by the wave
 140 farm in the three sea level rise scenarios, are investigated in this section. More
 141 specifically, the ratio of the value of $H_{s,br}$ with the farm to that without the farm
 142 (baseline), hereafter referred to as the wave height ratio. The wave farm reduces
 143 the significant wave height at breaking in all cases (Fig. 4). This reduction is
 144 more significant in the case of the easterly storm than for the westerly storm:
 145 alongshore-averaged ratios range between 0.79 and 0.8 in the three sea level rise
 146 scenarios for the easterly storm (Fig. 4b), far smaller than those for the westerly
 147 storm, 0.97 - 0.98 (Fig. 4a).

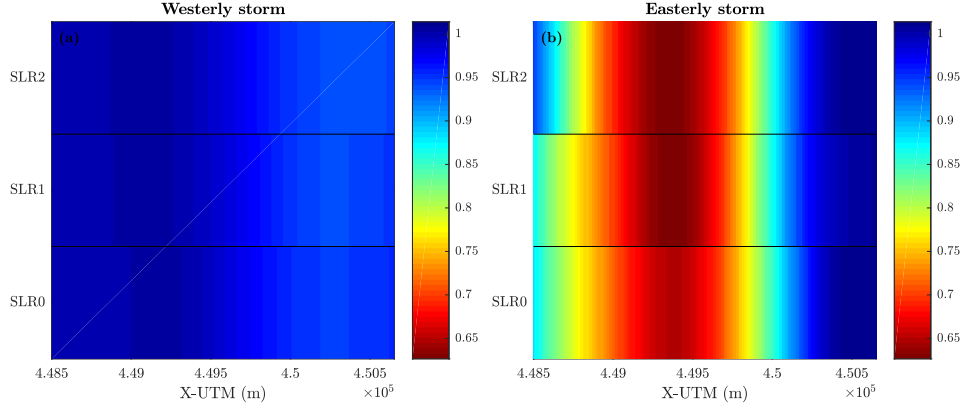


Figure 4: Ratio between the significant wave heights at breaking ($H_{s,br}$) with and without wave farm for the W (a) and E (b) storms.

When sea level rise is considered, the performance of the wave farm as coastal defence element improves slightly. In scenario SLR2, which has the largest sea level rise, the minimum wave height ratio for the westerly storm is 0.93. The corresponding values in scenarios SLR1 and SLR0 (baseline) are 0.94 and 0.95. In addition, with the increase in sea level, the shadow of the wave farm, i.e., the area of wave power deficit and consequently lower wave height, encompasses a greater length of coastline than in the baseline situation (Fig. 4). For the easterly storm, the differences between the optimistic and pessimistic projections for scenarios SLR1 and SLR2 are even smaller, with minimum wave height ratios of 0.63 in both cases. The minimum ratio rises up to 0.65 in SLR0.

4.2. LST rate variations

LST rates computed using the formulation of [59] are presented in this section. Sediment transport patterns are modified by the wave farm (Fig. 5). Under the westerly storm, these rates are reduced mainly in the eastern part of the study section, whereas the wave farm increases LST rates in the central part (Fig. 5a). Under the easterly storm, LST rates are reduced mainly in the central and western parts of Playa Granada, whereas the impact on the eastern end of the beach is lower (Fig. 5b). The differences between scenarios in the

166 eastern part of the beach under easterly storms are influenced by the effects
 167 of the shoreline horn (Punta del Santo, Fig. 2) on the propagation of easterly
 168 waves.

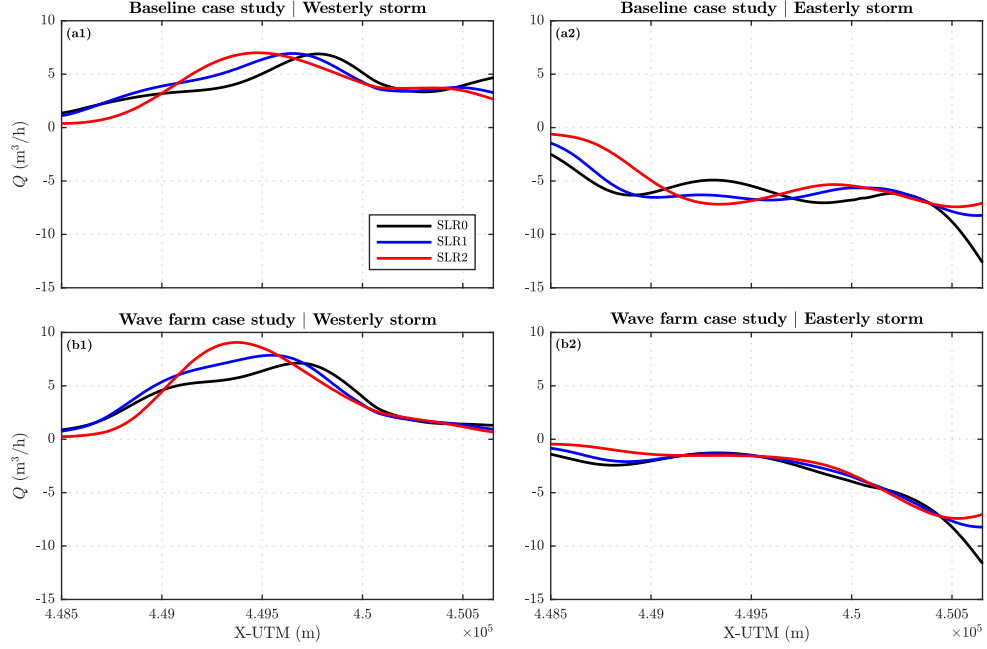


Figure 5: LST rate alongshore distribution without (a) and with (b) wave farm for the W (1) and E (2) storms.

169 This influence of the wave farm on LST patterns is readily analysed through
 170 the LST ratio, defined as the ratio between the LST rate with and without
 171 the wave farm (Figure 6). As described in the previous paragraph, under the
 172 westerly storm LST rates are increased in the central part, where maximum
 173 LST ratios of 1.53, 1.46, 1.45 are attained in scenarios SLR0, SLR1 and SLR2,
 174 respectively. On the contrary, in the western part of the beach the wave farm
 175 reduces LST rates, with minimum LST ratios as low as 0.28, 0.29 and 0.26,
 176 respectively (Fig. 6a). Sea level rise affects LST much as it does breaking
 177 wave heights, slightly increasing the positive impact of the wave farm; indeed,
 178 the alongshore-averaged LST ratio is higher in scenario SLR0 (0.95) than in
 179 scenarios SLR1 (0.93) and SLR2 (0.92).

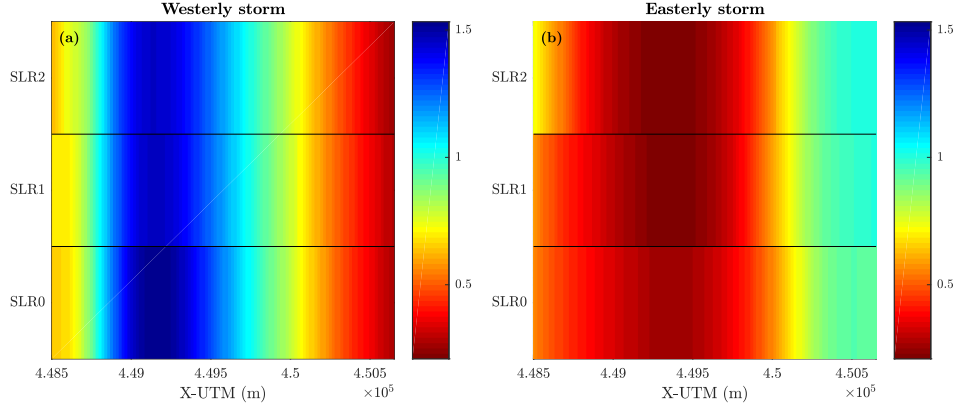


Figure 6: Ratio between the LST rates (Q) with and without wave farm for the W (a) and E (b) storms.

180 The modelled wave farm has a more intense impact under easterly storms.
 181 The minimum ratios, which are found in the central and western parts of the
 182 stretch of coast, are 0.26, 0.21 and 0.21 in SLR0, SLR1, SLR2, respectively (Fig.
 183 6b). Conversely, in the eastern part of the beach, the impact is lower (ratios
 184 close to unity in the three sea level rise scenarios). This greater impact under
 185 the easterly storm is confirmed by the alongshore averaged ratios: 0.51, 0.50
 186 and 0.52 for SLR0, SLR1 and SLR2, respectively.

187 4.3. Shoreline changes

188 LST rates computed in the previous section were the basis to apply the
 189 one-line model and assess changes in the shoreline caused by the sea states
 190 considered. The storms were modelled with a duration of 48 hours. The westerly
 191 storm causes erosion in the western part of the coast, whereas accretion appears
 192 in the eastern part (Fig. 7a1). Sea level rise modifies this behaviour, increasing
 193 erosion in the western part and reducing the advance of the shoreline in the
 194 central stretch. Maximum accretion is decreased; however, the shoreline advance
 195 is higher in the east end.

196 The easterly storm produces accretion in both ends of Playa Granada, with
 197 erosion appearing in the central stretch (Fig. 7a2). In this case, sea level

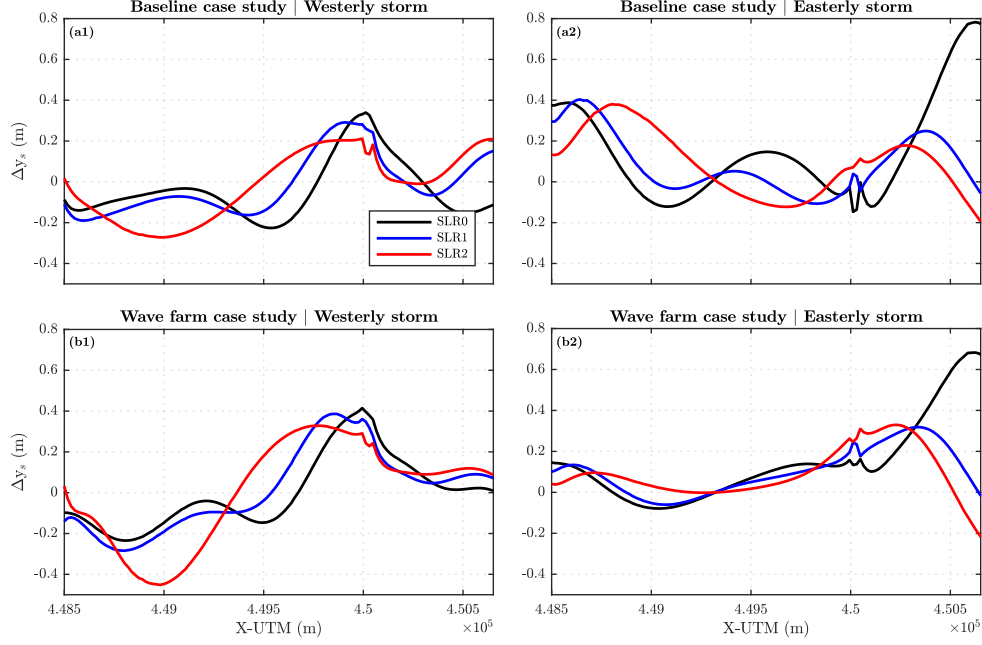


Figure 7: Shoreline advance (Δy_s) after 48 hours without (a) and with (b) wave farm for the westerly (1) and easterly (2) storms. Positive (negative) values mean accretion (erosion).

rise decreases erosion in the central part, turning it to accretion, especially in scenario SLR2. However, accretion in the easternmost part of the beach is decreased in the sea level rise scenarios. For both directions, the results around $X\text{-UTM} = 450000$ m are influenced by the changes in LST patterns and conditioned by the derivative in Eq. 2.

In order to quantify the effect of the wave farm on the variation of the shoreline, the non-dimensional shoreline advance [53] was computed. This indicator can be expressed as:

$$v = \frac{\Delta y_s - \Delta y_{s0}}{\max(|\Delta y_{s0}|)}, \quad (3)$$

with Δy_s and Δy_{s0} the variation in the shoreline position with and without wave farm. Positive and negative values indicate accretion or erosion, i.e., advance or retreat of the shoreline, respectively.

The wave farm produces erosion in a narrow zone in the western part of the beach, and accretion in the central and eastern parts of Playa Granada

211 under the westerly storm (Fig. 8a). It is clear on the graph that sea level rise
 212 enhances the impact of the wave farm. In the case of the erosion, the minimum
 213 non-dimensional shoreline advance in scenario SLR0 is equal to -0.46 , whereas
 214 in scenarios SLR1 and SLR2 this value is -0.54 and -0.57 , respectively – in
 215 other words, erosion (shoreline retreat) is more pronounced. A similar effect
 216 may be observed for the accretion (shoreline advance), with maximum values
 217 increasing from 0.51 in scenario SLR0 to 0.56 and 0.61 in scenarios SLR1 and
 218 SLR2, respectively. Taking into account the whole stretch of coast, accretion due
 219 to the presence of the wave farm dominates, with alongshore-averaged values of
 220 v equal to 0.11 , 0.10 and 0.09 for scenarios SLR0, SLR1 and SLR2, respectively.

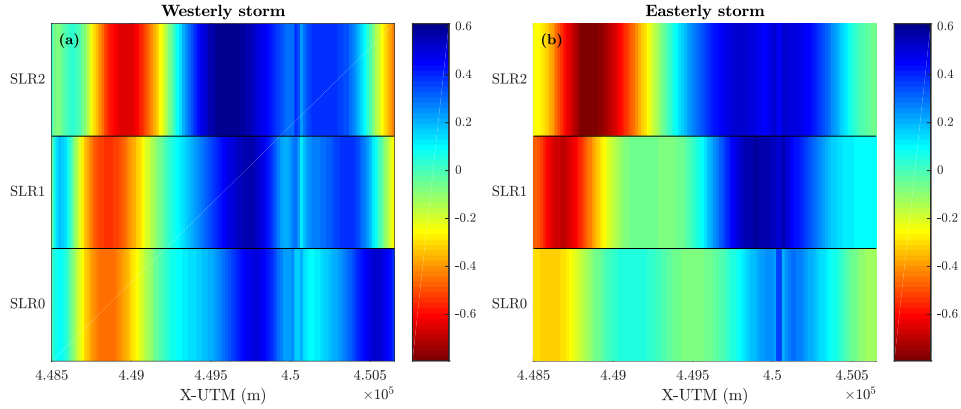


Figure 8: Non-dimensional shoreline advance (v) for the W (a) and E (b) storms. Positive (negative) values signify accretion (erosion).

221 Under the easterly storm, a similar impact is produced by the presence of
 222 the wave farm, with erosion again in the western part and accretion growing
 223 to the east (Fig. 8b). The effect of sea level rise, strengthening the impact –
 224 whether positive or negative – of the wave farm, is confirmed. Attending to the
 225 erosion in the western end, the minimum value of v in scenario SLR0 is -0.33 ,
 226 decreasing to -0.69 and -0.79 in scenarios SLR1 and SLR2, respectively. Like
 227 erosion, accretion is enhanced by the wave farm, with maximum values ranging
 228 from 0.35 in scenario SLR0 to 0.57 and 0.52 in scenarios SLR1 and SLR2,

229 respectively. The alongshore-averaged values of v under the easterly storm are
 230 lower: 0.001, 0.035 and 0.003 for scenarios SLR0, SLR1 and SLR2, respectively.

231 4.4. Subaerial beach area variation

232 The final subaerial beach area obtained for the different sea level rise sce-
 233 narios and the impact produced by the wave farm are presented in this section.
 234 Under the westerly storm, the wave farm produces a positive impact in terms of
 235 dry beach area. Erosion dominates without the wave farm in the three sea level
 236 rise scenarios, with subaerial beach area variations after 48 hours of: -90.15
 237 m^2 , -42.83 m^2 and -51.66 m^2 for scenarios SLR0, SLR1 and SLR2, respectively
 238 (Fig. 9a). With the presence of the wave farm, this erosion turns into accretion:
 239 $\Delta A = 2.31 \text{ m}^2$, $\Delta A = 28.76 \text{ m}^2$ and $\Delta A = 8.14 \text{ m}^2$ in scenarios SLR0, SLR1
 240 and SLR2, respectively. As may be observed in these results, sea level rise de-
 241 creases erosion without the wave farm, with lower beach area differences, and
 242 strengthens the accretionary effect of the wave farm, thus increasing the final
 243 subaerial beach area.

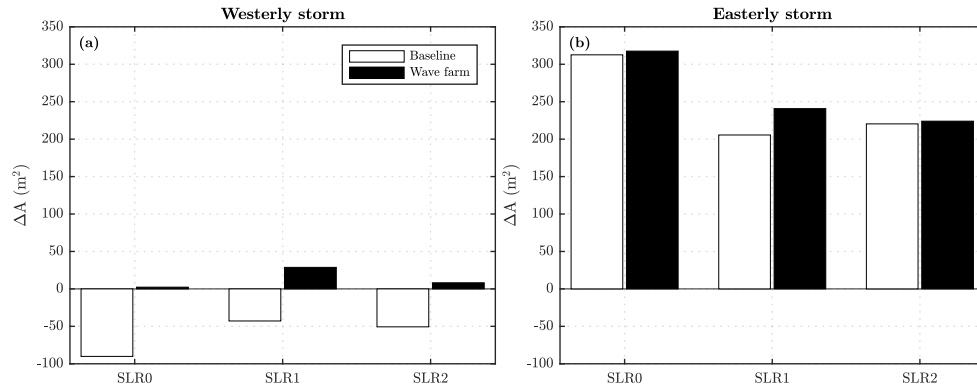


Figure 9: Subaerial beach area variation (ΔA) after 48 hours without (baseline) and with wave farm for the W (a) and E (b) storms.

244 The behaviour of the system is accretionary under the easterly storm (Fig.
 245 9b), as shown by the subaerial beach area difference in scenario SLR0 without
 246 wave farm (312.6 m^2). The results depict that this accretion will be attenuated

247 by sea level rise, decreasing the area differences to 205.55 m² and 220.38 m² in
248 scenarios SLR1 and SLR2, respectively. The wave farm would help to mitigate
249 these effects, increasing accretion in every scenario: 317.56 m² (SLR0), 240.74
250 m² (SLR1) and 224 m² (SLR2).

251 However, the effect of sea level rise on the beach cannot be fully understood
252 attending only to its impact on the LST and neglecting the loss of subaerial
253 beach area due to the coastal flooding resulting directly from the sea level rise.
254 Figure 10 depicts the total area of Playa Granada in every scenario studied.
255 The subaerial area available in the present situation is 101771 m². This area is
256 reduced to 88540 m² and 82679 m² in scenarios SLR1 and SLR2, respectively.
257 This means that 13231 m² will be lost by 2010 according to the optimistic pro-
258 jection, whereas this loss would rise to 19092 m² for the pessimistic projection.

259 The final subaerial beach area after the westerly storm for scenario SLR0
260 decreases to 101685 m², whereas the wave farm increases this area slightly to
261 101775 m². Under the easterly storm, the final area for this scenario with
262 (without) wave farm is 102073 m² (102061 m²). In scenario SLR1, the final
263 area with (without) wave farm under the westerly storm is 88570 m² (88497
264 m²) under the westerly storm and 88779 m² (88741 m²) under the easterly
265 one. Finally, the final area for the pessimistic projection (scenario SLR2) with
266 (without) wave farm is 82685 m² (82624 m²) under the westerly storm and
267 82906 m² (82900 m²) under the easterly storm.

268 These results show that due to sea level rise, between 13% and 19% of the
269 subaerial beach surface will be lost by 2100. In all the scenarios considered, the
270 effect of the wave farm is to increase the final subaerial beach area.

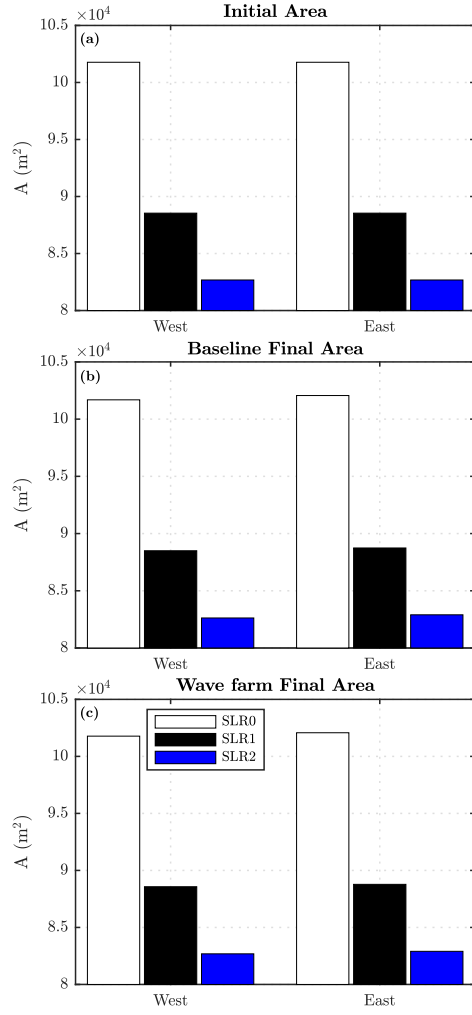


Figure 10: Initial and final subaerial beach area for the three sea level rise scenarios without and with wave farm.

271 5. Discussion

272 A number of research works have dealt with the coastal protection perfor-
273 mance provided by wave farms. For sandy beaches, [50–52] studied the effects
274 of wave farms on the beach profile in a storm scale. In the case of gravel dom-
275 inated beaches, recent works have studied the influence of different parameters
276 and conditions such as the alongshore position [54] or the wave farm layout
277 [53, 57]. However, none of these works have studied the repercussions of sea
278 level rise on the coastal protection against erosion provided by a wave farm,
279 which is the main motivation of this study.

280 The significance of this work lies in the fact that the results highlight the
281 efficiency of wave farms in coastal protection even in a sea level rise context. In
282 this manner, dual wave farms – for carbon-free energy generation and coastal
283 defence against erosion – become more attractive, since they can contribute to
284 two of the major challenges of the 21st century: the decarbonisation of the
285 energy mix and the mitigation of the impacts of climate change. This fact
286 enhances their interest as coastal defence elements against traditional hard-
287 engineering solutions, such as groynes or seawalls, which are not able to maintain
288 the same efficiency under a sea level rise conditions.

289 However, further research is required in this field. To fully take into account
290 the effects of sea level rise, research efforts focused on addressing the sea level
291 rise implications in coastal protection in the long-term scale are required.

292 6. Conclusions

293 Climate change has repercussions for the world’s coastlines, notably through
294 sea level rise and consequent erosion. Recent works have proposed the use of
295 wave farms with a dual purpose: carbon-free energy generation and coastal
296 protection. This work investigated the effects of a so-called dual wave farm on
297 a gravel-dominated beach and, for the first time, considered how these effects
298 were themselves modified by sea level rise. Using a spectral wave propagation
299 model (SWAN), a LST formulation and a one-line model, the final position of

the shoreline and final subaerial beach areas were calculated for three sea level rise scenarios: present situation (SLR0), and optimistic (SLR1) and pessimistic (SLR2) projections.

The presence of the wave farm reduces the significant wave height at breaking, with alongshore-averaged ratios with respect to the no-wave farm situation of 0.79 - 0.80 (0.97 - 0.98) for the easterly (westerly) storm. Sea level rise enhances the coastal protection efficiency of the wave farm by reducing the minimum ratios.

The reduction in significant wave height at breaking caused by the wave farm leads to a reduction in LST rates, with alongshore-averaged ratios with respect to the no-wave farm situation of 0.92 - 0.95 (0.51 - 0.52) for the westerly (easterly) storm. Sea level rise contributes to this positive effect of the wave farm, reducing the ratios of alongshore-averaged LST rates, especially for the westerly storm.

The shoreline shows accretion in the eastern part of the beach due to the presence of the wave farm, for both the westerly and easterly storms. However, some erosion appears in the western end. If the final (post-storm) subaerial beach area is considered, the effect of the wave farm is positive, i.e., accretionary. In the case of the westerly storm, the wave farm reverses the behaviour of the coast from an erosive to an accretionary response in every sea level rise scenario. Without the wave farm the subaerial beach area differences are -90.15 m^2 , -42.83 m^2 and -51.66 m^2 for scenarios SLR0, SLR1 and SLR2, respectively; with the wave farm these differences are 2.31 m^2 , 28.76 m^2 and 8.14 m^2 . Under the easterly storm, the coastal response is accretionary, and this behaviour is strengthened by the wave farm.

Acknowledgements

This paper was supported by the research grants WAVEIMPACT (PCIG-13-GA-2013-618556, European Commission, Marie Curie fellowship, fellow GI) and ICE (Intelligent Community Energy, European Commission, Contract no.

5025). RB was partly funded by the Spanish Ministry of Science, Innovation
 and Universities (*Programa Juan de la Cierva 2017*, FJCI-2017-31781). Wave
 and bathymetric data were provided by *Puertos del Estado* (Spain) and the
 Spanish Ministry of Agriculture, Fisheries and Food, respectively. We thank
 two anonymous reviewers for their improvements to this work.

References

- [1] B. Atilgan, A. Azapagic, Life cycle environmental impacts of electricity
 from fossil fuels in Turkey, *Journal of Cleaner Production* 106 (2015) 555–
 564.
- [2] Y. Achawangkul, N. Maruyama, M. Hirota, C. Chaichana, S. Sedpho,
 T. Sutabutr, Evaluation on environmental impact from the utilization of
 fossil fuel, electricity and biomass producer gas in the double-chambered
 crematories, *Journal of Cleaner Production* 134 (2016) 463–468.
- [3] P. K. Wesseh Jr, B. Lin, Options for mitigating the adverse effects of fossil
 fuel subsidies removal in Ghana, *Journal of Cleaner Production* 141 (2017)
 1445–1453.
- [4] F. Dalir, M. S. Motlagh, K. Ashrafi, A dynamic quasi comprehensive model
 for determining the carbon footprint of fossil fuel electricity: A case study
 of Iran, *Journal of Cleaner Production* 188 (2018) 362–370.
- [5] Intergovernmental Panel on Climate Change, *Climate change 2014: syn-
 thesis report*, IPCC Geneva, Switzerland, 2014.
- [6] L. M. Abadie, Sea level damage risk with probabilistic weighting of IPCC
 scenarios: An application to major coastal cities, *Journal of Cleaner Pro-
 duction* 175 (2018) 582–598.
- [7] European Commission, *A European Strategic Energy Technology Plan
 (Set-Plan): Towards a low carbon future*, Brussels: Commission of the
 European Communities (2007).

- 356 [8] J. Huenteler, C. Niebuhr, T. S. Schmidt, The effect of local and global
357 learning on the cost of renewable energy in developing countries, *Journal*
358 *of Cleaner Production* 128 (2016) 6 – 21.
- 359 [9] P. Nie, Y. Chen, Y. Yang, X. Henry Wang, Subsidies in carbon finance for
360 promoting renewable energy development, *Journal of Cleaner Production*
361 139 (2016) 677 – 684.
- 362 [10] M. O. A. González, J. S. Gonalves, R. M. Vasconcelos, Sustainable devel-
363 opment: Case study in the implementation of renewable energy in Brazil,
364 *Journal of Cleaner Production* 142 (2017) 461 – 475.
- 365 [11] C. Kung, L. Zhang, M. Chang, Promotion policies for renewable energy
366 and their effects in taiwan, *Journal of Cleaner Production* 142 (2017) 965
367 – 975.
- 368 [12] R. Maqbool, Y. Sudong, Critical success factors for renewable energy
369 projects; empirical evidence from Pakistan, *Journal of Cleaner Produc-*
370 *tion* (2018).
- 371 [13] H. L. Mendonça, M. V. d. A. Fonseca, et al., Working towards a frame-
372 work based on mission-oriented practices for assessing renewable energy
373 innovation policies, *Journal of Cleaner Production* 193 (2018) 709–719.
- 374 [14] F. J. Ramírez, A. Honrubia-Escribano, E. Gómez-Lázaro, D. T. Pham,
375 The role of wind energy production in addressing the European renewable
376 energy targets: The case of Spain, *Journal of Cleaner Production* (2018).
- 377 [15] X. Ruhang, S. Zixin, T. Qingfeng, Y. Zhuangzhuang, The cost and mar-
378 ketability of renewable energy after power market reform in China: A re-
379 view, *Journal of Cleaner Production* 204 (2018) 409–424.
- 380 [16] T. N. Sequeira, M. S. Santos, Renewable energy and politics: A systematic
381 review and new evidence, *Journal of Cleaner Production* 192 (2018) 553–
382 568.

- [17] A. Sinha, M. Shahbaz, T. Sengupta, Renewable Energy Policies and Contradictions in Causality: A case of Next 11 Countries, *Journal of Cleaner Production* 197 (2018) 73–84.
- [18] R. Waheed, D. Chang, S. Sarwar, W. Chen, Forest, agriculture, renewable energy, and CO2 emission, *Journal of Cleaner Production* 172 (2018) 4231–4238.
- [19] X.-C. Yuan, Y.-J. Lyu, B. Wang, Q.-H. Liu, Q. Wu, China’s energy transition strategy at the city level: The role of renewable energy, *Journal of Cleaner Production* 205 (2018) 980–986.
- [20] A. Clément, P. McCullen, A. F. de O. Falcão, A. Fiorentino, F. Gardner, K. Hammarlund, G. Lemonis, T. Lewis, K. Nielsen, S. Petroncini, M.-T. Pontes, P. Schild, B.-O. Sjöström, H. C. Sørensen, T. Thorpe, Wave energy in Europe: current status and perspectives, *Renewable and Sustainable Energy Reviews* 6 (2002) 405–431.
- [21] A. M. Cornett, A global wave energy resource assessment, in: *The Eighteenth International Offshore and Polar Engineering Conference*, International Society of Offshore and Polar Engineers, 2008.
- [22] J. Cruz, *Ocean wave energy: current status and future perspectives*, Springer Science & Business Media, 2008.
- [23] A. F. de O. Falcão, Modelling and control of oscillating-body wave energy converters with hydraulic power take-off and gas accumulator, *Ocean Engineering* 34 (2007) 2021–2032.
- [24] P. Contestabile, C. Iuppa, E. D. Lauro, L. Cavallaro, T. L. Andersen, D. Vicinanza, Wave loadings acting on innovative rubble mound breakwater for overtopping wave energy conversion, *Coastal Engineering* 122 (2017) 60 – 74.

- [25] H. Fernandez, G. Iglesias, R. Carballo, A. Castro, J. Fraguela, F. Taveira-Pinto, M. Sanchez, The new wave energy converter WaveCat: Concept and laboratory tests, *Marine Structures* 29 (2012) 58–70.
- [26] I. López, B. Pereiras, F. Castro, G. Iglesias, Optimisation of turbine-induced damping for an OWC wave energy converter using a RANS–VOF numerical model, *Applied Energy* 127 (2014) 105 – 114.
- [27] E. Medina-López, R. Bergillos, A. Moñino, M. Clavero, M. Ortega-Sánchez, Effects of seabed morphology on oscillating water column wave energy converters, *Energy* 135 (2017) 659–673.
- [28] A. Moñino, E. Medina-López, R. J. Bergillos, M. Clavero, A. Borthwick, M. Ortega-Sánchez, *Thermodynamics and Morphodynamics in Wave Energy*, Springer, 2018.
- [29] E. Medina-López, A. Moñino, R. Bergillos, M. Clavero, M. Ortega-Sánchez, Oscillating water column performance under the influence of storm development, *Energy* 166 (2019) 765–774.
- [30] G. Iglesias, R. Carballo, Choosing the site for the first wave farm in a region: A case study in the Galician Southwest (Spain), *Energy* 36 (2011) 5525–5531.
- [31] R. Carballo, M. Sánchez, V. Ramos, J. Fraguela, G. Iglesias, The intra-annual variability in the performance of wave energy converters: A comparative study in N Galicia (Spain), *Energy* 82 (2015) 138 – 146.
- [32] M. López, M. Veigas, G. Iglesias, On the wave energy resource of Peru, *Energy Conversion and Management* 90 (2015) 34 – 40.
- [33] D. Silva, A. R. Bento, P. Martinho, C. G. Soares, High resolution local wave energy modelling in the Iberian Peninsula, *Energy* 91 (2015) 1099–1112.
- [34] A. Viviano, S. Naty, E. Foti, T. Bruce, W. Allsop, D. Vicinanza, Large-scale experiments on the behaviour of a generalised oscillating water column under random waves, *Renewable Energy* 99 (2016) 875 – 887.

- 437 [35] A. López-Ruiz, R. J. Bergillos, M. Ortega-Sánchez, The importance of
438 wave climate forecasting on the decision-making process for nearshore wave
439 energy exploitation, *Applied Energy* 182 (2016) 191–203.
- 440 [36] A. López-Ruiz, R. J. Bergillos, A. Lira-Loarca, M. Ortega-Sánchez, A
441 methodology for the long-term simulation and uncertainty analysis of the
442 operational lifetime performance of wave energy converter arrays, *Energy*
443 153 (2018) 126–135.
- 444 [37] A. López-Ruiz, R. J. Bergillos, J. M. Raffo-Caballero, M. Ortega-Sánchez,
445 Towards an optimum design of wave energy converter arrays through an
446 integrated approach of life cycle performance and operational capacity, *Ap-
447 plied Energy* 209 (2018) 20–32.
- 448 [38] C. Pérez-Collazo, D. Greaves, G. Iglesias, A review of combined wave and
449 offshore wind energy, *Renewable and Sustainable Energy Reviews* 42 (2015)
450 141 – 153.
- 451 [39] S. Astariz, C. Perez-Collazo, J. Abanades, G. Iglesias, Towards the optimal
452 design of a co-located wind-wave farm, *Energy* 84 (2015) 15 – 24.
- 453 [40] S. Astariz, J. Abanades, C. Perez-Collazo, G. Iglesias, Improving wind farm
454 accessibility for operation and maintenance through a co-located wave farm:
455 Influence of layout and wave climate, *Energy Conversion and Management*
456 95 (2015) 229 – 241.
- 457 [41] P. Contestabile, E. Di Lauro, M. Buccino, D. Vicinanza, Economic As-
458 sessment of Overtopping BReakwater for Energy Conversion (OBREC): A
459 Case Study in Western Australia, *Sustainability* 9 (2016).
- 460 [42] S. Astariz, G. Iglesias, The economics of wave energy: A review, *Renewable
461 and Sustainable Energy Reviews* 45 (2015) 397 – 408.
- 462 [43] S. Astariz, A. Vazquez, G. Iglesias, Evaluation and comparison of the
463 levelized cost of tidal, wave, and offshore wind energy, *Journal of Renewable
464 and Sustainable Energy* 7 (2015) 053112.

- [44] S. Astariz, G. Iglesias, Wave energy vs. other energy sources: A reassessment of the economics, *International Journal of Green Energy* 13 (2016) 747–755.
- [45] M. I. Vousedoukas, L. Mentaschi, E. Voukouvalas, A. Bianchi, F. Dottori, L. Feyen, Climatic and socioeconomic controls of future coastal flood risk in Europe, *Nature Climate Change* 8 (2018) 776–780.
- [46] M. I. Vousedoukas, L. Mentaschi, E. Voukouvalas, M. Verlaan, S. Jevrejeva, L. P. Jackson, L. Feyen, Global probabilistic projections of extreme sea levels show intensification of coastal flood hazard, *Nature Communications* 9 (2018) 2360.
- [47] J. M. Sayol, M. Marcos, Assessing Flood Risk Under Sea Level Rise and Extreme Sea Levels Scenarios: Application to the Ebro Delta (Spain), *Journal of Geophysical Research: Oceans* 123 (2018) 794–811.
- [48] E. J. Anthony, N. Marriner, C. Morhange, Human influence and the changing geomorphology of Mediterranean deltas and coasts over the last 6000 years: From progradation to destruction phase?, *Earth-Science Reviews* 139 (2014) 336–361.
- [49] J. P. M. Syvitski, A. J. Kettner, I. Overeem, E. W. H. Hutton, M. T. Hannon, G. R. Brakenridge, J. Day, C. Vörösmarty, Y. Saito, L. Giosan, R. J. Nicholls, Sinking deltas due to human activities, *Nature Geoscience* 2 (2009) 681–686.
- [50] J. Abanades, D. Greaves, G. Iglesias, Coastal defence through wave farms, *Coastal Engineering* 91 (2014) 299–307.
- [51] J. Abanades, D. Greaves, G. Iglesias, Wave farm impact on the beach profile: A case study, *Coastal Engineering* 86 (2014) 36–44.
- [52] J. Abanades, D. Greaves, G. Iglesias, Wave farm impact on beach modal state, *Marine Geology* 361 (2015) 126–135.

- 492 [53] C. Rodriguez-Delgado, R. J. Bergillos, M. Ortega-Sánchez, G. Iglesias, Pro-
493 tection of gravel-dominated coasts through wave farms: Layout and shore-
494 line evolution, *Science of The Total Environment* 636 (2018) 1541 – 1552.
- 495 [54] C. Rodriguez-Delgado, R. J. Bergillos, M. Ortega-Sánchez, G. Iglesias,
496 Wave farm effects on the coast: The alongshore position, *Science of The*
497 *Total Environment* 640-641 (2018) 1176 – 1186.
- 498 [55] R. J. Bergillos, A. López-Ruiz, E. Medina-López, A. Moñino, M. Ortega-
499 Sánchez, The role of wave energy converter farms on coastal protection in
500 eroding deltas, Guadalfeo, southern Spain, *Journal of Cleaner Production*
501 171 (2018) 356 – 367.
- 502 [56] R. J. Bergillos, C. Rodriguez-Delgado, G. Iglesias, Wave farm impacts on
503 coastal flooding under sea-level rise: a case study in southern Spain, *Science*
504 *of the Total Environment*, 653 (2019) 1522–1531.
- 505 [57] C. Rodriguez-Delgado, R. J. Bergillos, G. Iglesias, Dual wave farms and
506 coastline dynamics: The role of inter-device spacing, *Science of The Total*
507 *Environment* 646 (2019) 1241 – 1252.
- 508 [58] J. Abanades, G. Flor-Blanco, G. Flor, G. Iglesias, Dual wave farms for
509 energy production and coastal protection, *Ocean & Coastal Management*
510 160 (2018) 18 – 29.
- 511 [59] L. C. van Rijn, A simple general expression for longshore transport of sand,
512 gravel and shingle, *Coastal Engineering* 90 (2014) 23 – 39.
- 513 [60] R. Pelnard-Considère, Essai de theorie de l’évolution des formes de rivage
514 en plages de sable et de galets, *Les Energies de la Mer: Compte Rendu*
515 *Des Quatriemes Journees de L’hydraulique*, Paris 13, 14 and 15 Juin 1956;
516 Question III, rapport 1, 74-1-10 (1956).
- 517 [61] R. J. Bergillos, C. Rodríguez-Delgado, A. López-Ruiz, A. Mil-
518 lares, M. Ortega-Sánchez, M. A. Losada, Recent human-induced

- 519 coastal changes in the Guadalfeo river deltaic system (southern
520 Spain), in: Proceedings of the 36th IAHR-International Association
521 for Hydro-Environment Engineering and Research World Congress:
522 <http://89.31.100.18/~iahrpapers/87178.pdf>, 2015.
- [62] 523 R. J. Bergillos, M. Ortega-Sánchez, M. A. Losada, Foreshore evolution
524 of a mixed sand and gravel beach: The case of Playa Granada (Southern
525 Spain), in: Proceedings of the 8th Coastal Sediments, World Scientific,
526 2015.
- [63] 527 R. J. Bergillos, M. Ortega-Sánchez, G. Masselink, M. A. Losada, Morpho-
528 sedimentary dynamics of a micro-tidal mixed sand and gravel beach, Playa
529 Granada, southern Spain, *Marine Geology* 379 (2016) 28–38.
- [64] 530 R. J. Bergillos, G. Masselink, R. T. McCall, M. Ortega-Sánchez, Mod-
531 elling overwash vulnerability along mixed sand-gravel coasts with XBeach-
532 G: Case study of Playa Granada, southern Spain, in: Coastal Engineering
533 Proceedings, volume 1 (35), 2016, p. 13.
- [65] 534 R. J. Bergillos, C. Rodríguez-Delgado, A. Millares, M. Ortega-Sánchez,
535 M. A. Losada, Impact of river regulation on a mediterranean delta: Assess-
536 ment of managed versus unmanaged scenarios, *Water Resources Research*
537 52 (2016) 5132–5148.
- [66] 538 R. J. Bergillos, M. Ortega-Sánchez, Assessing and mitigating the landscape
539 effects of river damming on the Guadalfeo River delta, southern Spain,
540 *Landscape and Urban Planning* 165 (2017) 117–129.
- [67] 541 R. J. Bergillos, C. Rodríguez-Delgado, M. Ortega-Sánchez, Advances in
542 management tools for modeling artificial nourishments in mixed beaches,
543 *Journal of Marine Systems* 172 (2017) 1–13.
- [68] 544 R. J. Bergillos, A. López-Ruiz, D. Principal-Gómez, M. Ortega-Sánchez, An
545 integrated methodology to forecast the efficiency of nourishment strategies
546 in eroding deltas, *Science of the Total Environment* 613 (2018) 1175–1184.

- 547 [69] M. Ortega-Sánchez, R. J. Bergillos, A. López-Ruiz, M. A. Losada, Mor-
548 phodynamics of Mediterranean Mixed Sand and Gravel Coasts, Springer,
549 2017.
- 550 [70] R. J. Bergillos, G. Masselink, M. Ortega-Sánchez, Coupling cross-shore
551 and longshore sediment transport to model storm response along a mixed
552 sand-gravel coast under varying wave directions., Coastal Engineering, 129
553 (2017) 93–104.
- 554 [71] R. J. Bergillos, A. López-Ruiz, M. Ortega-Sánchez, G. Masselink, M. A.
555 Losada, Implications of delta retreat on wave propagation and longshore
556 sediment transport-Guadalejo case study (southern Spain), Marine Geol-
557 ogy 382 (2016) 1–16.
- 558 [72] G. Iglesias, R. Carballo, A. Castro, B. Fraga, Development and design of
559 the WaveCatTM energy converter, in: Coastal Engineering 2008: (In 5
560 Volumes), World Scientific, 2009, pp. 3970–3982.
- 561 [73] G. Iglesias, H. Fernández, R. Carballo, A. Castro, F. Taveira-Pinto, The
562 wavecat©-development of a new wave energy converter, in: World Re-
563 newable Energy Congress-Sweden; 8-13 May; 2011; Linköping; Sweden, 57,
564 Linköping University Electronic Press, 2011, pp. 2151–2158.
- 565 [74] G. Iglesias, R. Carballo, A. Castro, B. Fraga, Development and design of
566 the WaveCatTM energy converter, in: Coastal Engineering 2008: (In 5
567 Volumes), World Scientific, 2009, pp. 3970–3982.
- 568 [75] R. Carballo, G. Iglesias, Wave farm impact based on realistic wave-WEC
569 interaction, Energy 51 (2013) 216–229.
- 570 [76] H. Fernandez, G. Iglesias, R. Carballo, A. Castro, M. Sánchez, F. Taveira-
571 Pinto, Optimization of the wavecat wave energy converter, Coastal Engi-
572 neering Proceedings 1 (2012) 5.
- 573 [77] L. Holthuijsen, N. Booij, R. Ris, A spectral wave model for the coastal
574 zone, ASCE, 1993.

- 575 [78] E. Rusu, C. G. Soares, Coastal impact induced by a Pelamis wave farm
576 operating in the Portuguese nearshore, *Renewable Energy* 58 (2013) 34–49.
- 577 [79] A. Kieftenburg, A short overview of reflection formulations and suggestions
578 for implementation in SWAN, Technical Report, TU Delft, Department of
579 Hydraulic Engineering, 2001.